

Theory of Electronic Noise in Semiconductor Materials and Devices

Lino Reggiani

Dipartimento di Fisica ed Istituto Nazionale di Fisica della Materia, Università di Modena, Via Campi 213/A, 41100 Modena, Italy

Luca Varani

Centre d'Electronique de Montpellier, Université Montpellier II, 34095 Montpellier Cedex 5, France

Tilman Kuhn

Institut für Theoretische Physik, Universität Stuttgart, Pfaffenwaldring 57, 70550 Stuttgart, Germany

Tomás González, Daniel Pardo

Departamento de Física Aplicada, Universidad de Salamanca, Plaza de la Merced s/n, 37008 Salamanca, Spain

ABSTRACT — We present a microscopic theory of electronic noise in semiconductor two-terminal devices which is based on Monte Carlo simulations of the carrier motion self-consistently coupled with a Poisson solver. Current and voltage noise operations are applied and their respective representations discussed. As application we consider the cases of resistors, n^+nn^+ structures, and Schottky-barrier diodes. Phenomena associated with coupling between fluctuations in carrier velocity and self-consistent electric field are quantitatively investigated for the first time. At increasing applied fields, hot-carrier effects are found to be relevant importance in all the cases considered here.

RIASSUNTO — Viene presentata una teoria microscopica del rumore elettrico in dispositivi a semiconduttore a due terminali, basata su simulazioni Monte Carlo dei portatori, accoppiate in modo consistente con un solutore dell'equazione di Poisson. Si sono svolti e discussi calcoli su corrente e tensione di rumore. Come applicazione si sono studiati resistori, giunzioni n^+nn^+ e diodi a barriera Schottky. Per la prima volta sono stati studiati quantitativamente i fenomeni di accoppiamento tra fluttuazione della velocità e campo elettrico autoconsistente. In tutte le situazioni considerate si è trovato che al crescere del campo elettrico applicato diventano importanti gli effetti legati ai portatori caldi.

1. Introduction

In this communication we present some relevant results of a microscopic theory for electronic noise in semiconductor materials and devices. To this end, we make use of the Monte Carlo (MC) technique /1/ which, by naturally incorporating all the microscopic noise sources, has recently emerged as a very powerful method /2/. Systems with increasing degree of complexity are investigated for illustrative purposes.

2. Theory

The primary quantity which describes electronic noise is the spectral density of current (voltage) fluctuations $S_I(f)$ ($S_V(f)$). It can be measured more or less directly in different ranges of the frequency f and microscopically interpreted from the calculation of its theoretical counterpart which is the associated correlation function $C_I(t)$ ($C_V(t)$). The determination of the current (voltage) correlation function is performed from the knowledge of the time series $I(t)$ ($\Delta V(t)$) as calculated from an ensemble MC simulation eventually coupled with a self-consistent Poisson solver, and taking appropriate boundary conditions concerning carrier injection-ex-

traction from the contacts of the device. To this end, the total simulation, neglecting the initial transient, is recorded on a time-grid of step-size Δt . Then, by defining the time length in which the correlation function should be calculated as $m\Delta t$, with m integer, the correlation function $C_X(t)$ ($X = I, \Delta V$) is obtained as:

$$C_X(j\Delta t) = \overline{X(t')X(t'+j\Delta t)} = \frac{1}{M-m} \sum_{i=1}^{M-m} X(i\Delta t)X[(i+j)\Delta t] \quad (1)$$

with $j = 0, 1, \dots, m$; $M > m$. Typical values are: $M = 50m$, $m = 100$. The corresponding $S_X(f)$ is determined by Fourier transformation. Unless otherwise stated, in the following we consider periodic boundary conditions at the contacts, thus fulfilling the neutrality condition for the whole device at any time. This condition is well verified provided the length of the active region of the device is longer than the Debye length.

3. Applications

In this Section we report results obtained by the MC technique as applied to different systems with increasing degree of complexity.

3.1 Resistors

The system we consider is a submicron Si resistor of length $L = 0.6 \mu\text{m}$ with a donor concentration of 10^{17}cm^{-3} at 300K /3/. Figure 1 shows the current correlation function calculated at increasing applied voltages where its faster decay is associated with the onset of hot-carrier conditions. The presence of a negative part in $C_I(t)$ is attributed to the coupling between energy and velocity relaxation processes /4/. Figure 2 shows the voltage correlation functions $C_V(t)$ for the same resistor. At low voltages plasma and differential dielectric-relaxation times are responsible for the oscillatory and dumping behaviors, respectively. At increasing applied voltages the subohmic behavior of the current-voltage characteristics implies a significant increase of the dielectric relaxation time which, by becoming longer than the plasma time, washes-out the oscillations.

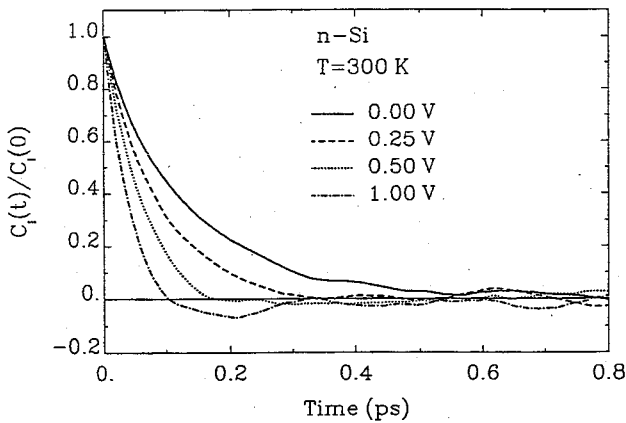


Fig. 1 - Autocorrelation functions of current fluctuations for the different applied voltages reported. Calculations refers to a Si homogeneous structure with $n = 10^{17} \text{cm}^{-3}$ $L = 0.6 \mu\text{m}$, at $T = 300\text{K}$.

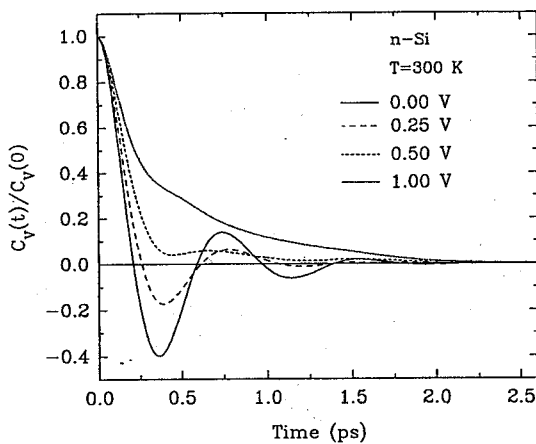


Fig. 2 - Autocorrelation function of voltage fluctuations in the same structure and conditions as Fig. 1.

3.2 n^+nn^+ structures

The system we consider is a submicron Si n^+nn^+ structure at 300K with two abrupt homojunctions along the x -direction /3/. The lengths of the three regions are indicated respectively as L_1, L and L_2 . Figure 3 shows the current correlation function for a structure with $L = L_1 = L_2 = 0.2 \mu\text{m}$. The total correlation function can be decomposed as the sum of a diagonal and off-diagonal contribution /4/. The former, by giving the autocorrelation of the single particle-velocity, is responsible for the exponential decay. The latter, being associated with the long-range Coulomb interaction, is responsible for an oscillatory behavior related to the plasma frequency of the n^+ and n regions.

Figure 4 shows a 3-dimensional plot of the voltage corre-

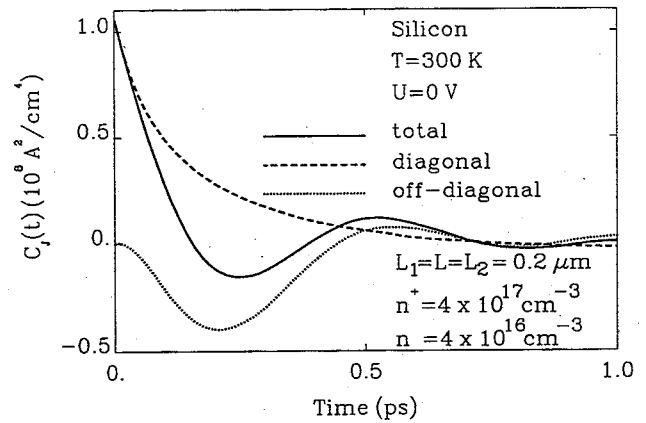


Fig. 3 - Autocorrelation function of current-density fluctuations at equilibrium for a Si n^+nn^+ structure at $T = 300\text{K}$ with $n^+ = 4 \times 10^{17} \text{cm}^{-3}$, $n = 4 \times 10^{16} \text{cm}^{-3}$, and length $0.20-0.20-0.20 \mu\text{m}$, respectively. Continuous, dashed and dotted curves refer respectively to the total, diagonal and off-diagonal terms /5/.

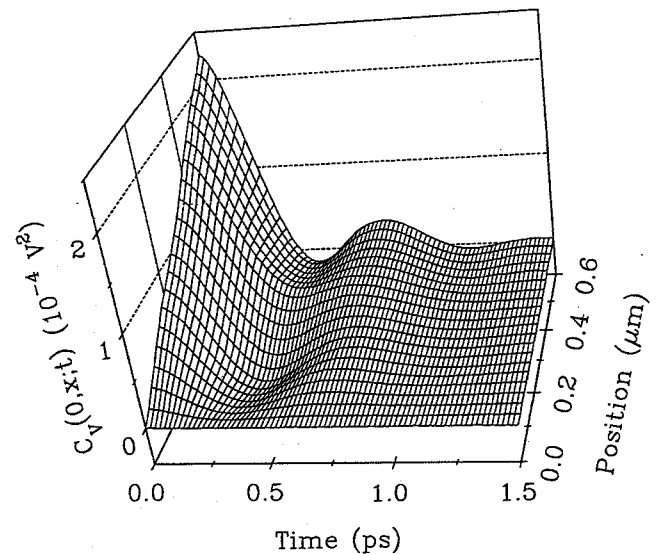


Fig. 4 - Autocorrelation function of voltage fluctuations as a function of time and position at equilibrium for a Si n^+nn^+ structure at $T = 300\text{K}$ with $n^+ = 10^{17} \text{cm}^{-3}$, $n = 10^{16} \text{cm}^{-3}$, and length $0.20-0.20-0.20 \mu\text{m}$, respectively.

lation-function $C_V(0,x;t)$ as obtained from Eq. (1) by considering the voltage drop between the left contact of the structure taken as origin and a sampling point at x in the range $0 \div (L_1+L+L_2)$ with $n = 10^{16}\text{cm}^{-3}$ and $n^+ = 10^{17}\text{cm}^{-3}$. The time evolution of $C_V(0,x;t)$ depends on the contribution to the voltage fluctuations which comes from each region in the structure through the value of its resistance and doping. In this way we observe that, through the plasma time, the n^+ regions are responsible for an oscillatory behavior that at increasing times is suppressed by dielectric relaxation/6/. In the n region the evolution is mainly determined by dielectric relaxation through a contribution which decreases exponentially

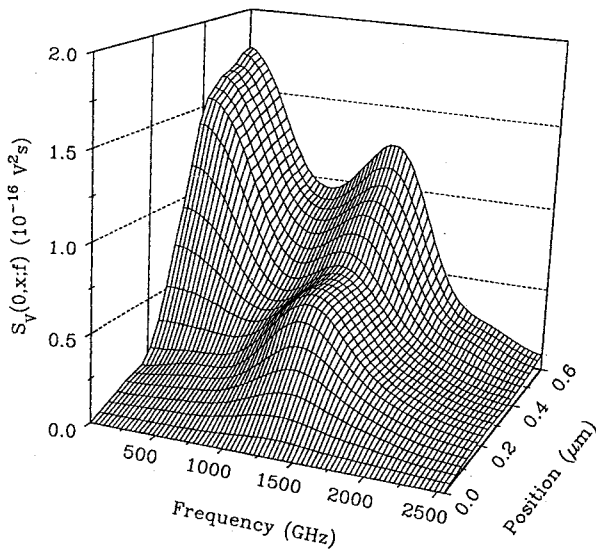


Fig. 5 - Spectral density of voltage fluctuations as a function of frequency and position at equilibrium in the same structure and conditions as Fig. 4.

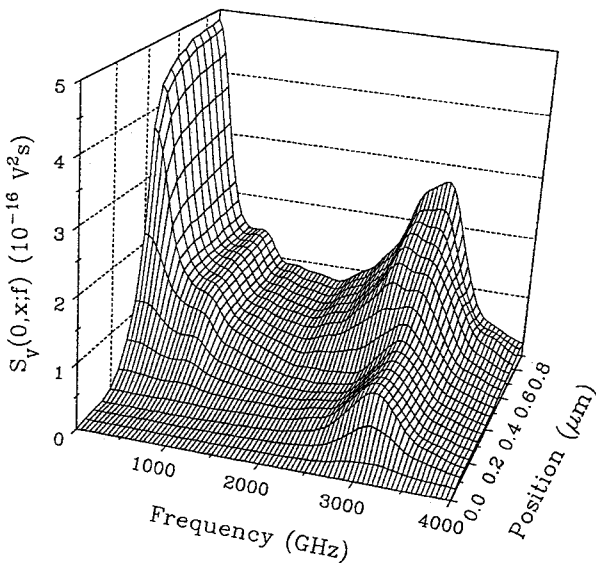


Fig. 6 - Spectral density of voltage fluctuations as a function of frequency and position in a GaAs n^+nn^+ structure for an average voltage $\Delta V(L) = 0.45\text{V}$ at $T = 300\text{K}$ with $n^+ = 10^{17}\text{cm}^{-3}$, $n = 10^{14}\text{cm}^{-3}$, and length $0.15-0.25-0.50\mu\text{m}$, respectively.

with time. It is remarkable the very good agreement found for $C_V(0,x;0) = K_B T x / (\epsilon_0 \epsilon_r A) / 7$, K_B being the Boltzmann constant, T the bath temperature, ϵ_0 the vacuum permittivity, ϵ_r the relative dielectric constant of the material and A the cross-sectional area of the sample.

Figure 5 shows the voltage spectral-density corresponding to Fig. 4.

Here, the different influence of each region in the structure is clearly emphasized. At low frequencies, most of the noise is originated in the n region due to its larger resistance. It is interesting to notice that the presence of the self-consistent field in the homojunctions produces some smoothing from the three-slope linear behavior which is expected for a simple series-resistance model $S_V(0,x;0) = 4K_B T R(0,x)$, where $R(0,x)$ is the ohmic resistance of the structure up to the point x . When going to higher frequencies, the contribution to the spectral density coming from the n region decreases, while that of the n^+ regions increases, reaching its maximum value for the associated plasma frequency (1275GHz). At this frequency it can be clearly observed that the only contribution to the spectral density comes from the n^+ regions.

Figure 6 shows the voltage spectral-density for a GaAs n^+nn^+ structure with $n^+ = 10^{17}\text{cm}^{-3}$, $n = 10^{14}\text{cm}^{-3}$ and length $0.15-0.25-0.50\mu\text{m}$, at $T = 300\text{K}$ with an average applied voltage of $0.45\text{V}/6$. Analogously to the case of Si, the structure exhibits a noticeable peak at the plasma frequency corresponding to the n^+ region. Furthermore, in the lowest frequency region the contribution of the drain region to noise is found to be of great importance. Indeed, here the presence of carriers in the higher satellite valleys implies a deeper penetration of hot carriers in the drain before they can thermalize. Therefore, this region becomes highly resistive and thus highly noisy. We remark the evidence of a minor peak at about 500GHz, the origin of which is attributed to the presence of $\Gamma-L$ intervalley mechanism in the vicinity of the second homojunction.

3.3 Schottky diodes

The system we consider is a one-dimensional GaAs n^+-n -metal structure at $300\text{K}/8$.

The doping of the n^+ region is 10^{17}cm^{-3} and it is $0.35\mu\text{m}$ long. At its left side, where the carriers are injected into the device, an ohmic contact is simulated, and the number of electrons considered is updated. The n region is $0.35\mu\text{m}$ long and its doping is 10^{16}cm^{-3} . At its end it is the Schottky barrier with the metal contact acting as a perfect absorbing boundary. The height of the barrier considered in the simulation is 0.735V , which leads to an effective built-in voltage between the n region of the semiconductor and the metal of 0.640V . The cross-sectional area adopted for the device is $2 \times 10^{-9}\text{cm}^2$, which means an average number of simulated carriers around 7600 depending on the bias.

Figure 7 shows $S_V(f)$ at increasing applied voltages where the current-voltage characteristic exhibits an exponential behavior. The complexity of the spectrum is understood on the basis of a strong coupling between fluctuations in carrier velocity and the self-consistent electric field. Two peaks are ob-

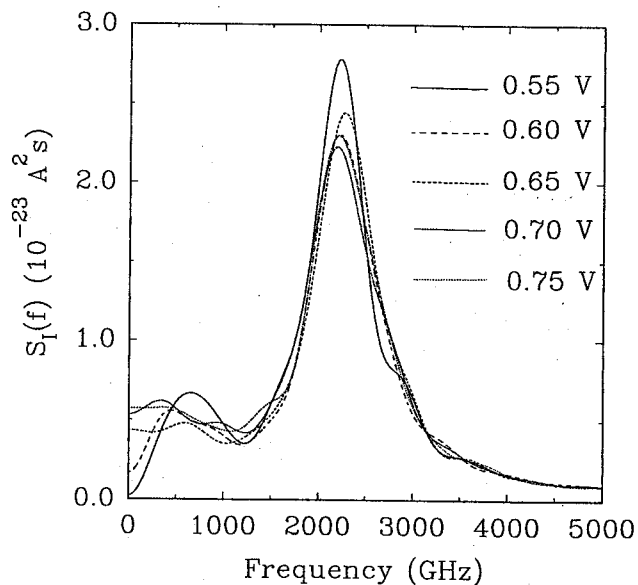


Fig. 7 - Current spectral-density as a function of frequency for a GaAs Schottky barrier diode at $T=300\text{K}$ with $n=10^{16}\text{cm}^{-3}$, $n^+=10^{17}\text{cm}^{-3}$ and length of each region of $0.35\mu\text{m}$. Different curves refer to the reported applied voltages.

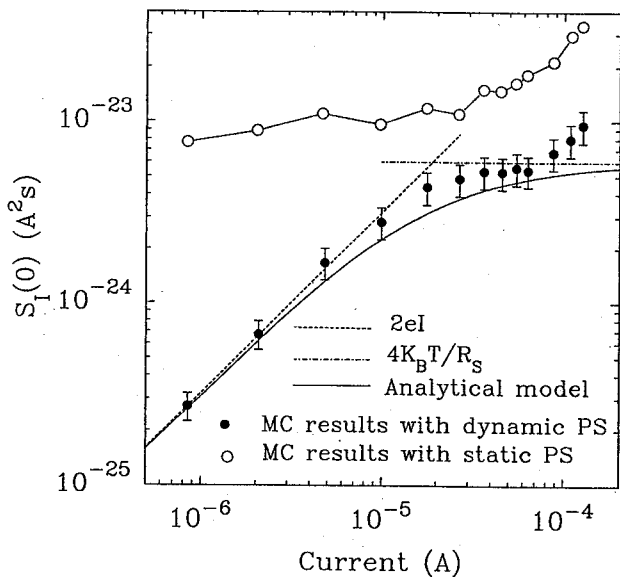


Fig. 8 - Low-frequency value of the spectral density of current fluctuations as a function of the current flowing through the same structure as Fig. 7. Symbols refer to MC calculations performed considering a dynamic (closed circles) and a static (open circles) Poisson solver, respectively, the continuous line to the analytical model from Eq. (2).

served, one in the region below 10^3GHz and another at about $2.2 \times 10^3\text{GHz}$. The first is attributed to carriers that have insufficient kinetic energy to surpass the barrier and return to the neutral semiconductor region, as explained in Ref. /9/. The second originates from the coupling between fluctuations in carrier velocity and in the self-consistent field due to the inhomogeneity introduced by the n^+-n homojunction/8/.

By reporting $S_I(0)$ as a function of the current, Fig. 8 en-

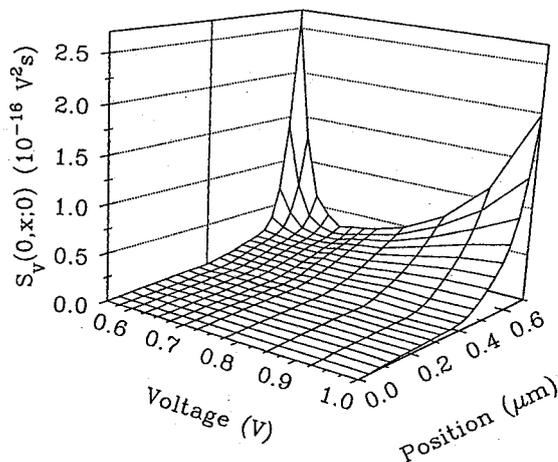


Fig. 9 - Low-frequency value of the spectral density of voltage fluctuations as a function of position and mean voltage in the same structure as Fig. 7.

ables an analysis of noise surces to be carried out. Accordingly, at low currents shot-noise /10/ is found to be dominant, so that $S_I(0)$ exhibits a $2eI$ dependence, e being the unit charge. At higher currents, $S_I(0)$ approaches a thermal noise behavior $S_I(0) = 4K_B T / R_s$, R_s being the differential series resistance, and finally exhibits a steep increase associated with hot-carrier effects. By considering the first two behaviors, $S_I(0)$ can be expressed as /9/:

$$S_I(0) = \frac{2eIR_j^2 + 4K_B TR_s}{(R_s + R_j)^2} \quad (2)$$

where R_j is the differential resistance of the junction space-charge region. In Fig. 8 the results of the simulation are favorably compared with this analytical model and the two limit behaviors. Figure 8 also reports the values obtained for $S_I(0)$ when a static Poisson solver is considered in the simulation by using the field profile corresponding to the stationary situation. While the static characteristics are checked to remain the same, the results for $S_I(0)$ differ considerably, and no transition from a shot-noise behavior to a thermal-noise behavior is noticed. These results prove the essential role played by the coupling between fluctuations in carrier velocity and self-consistent electric field in determining the noise spectra.

Figure 9 shows a spatial analysis of the low-frequency value of the voltage spectral density. For voltages lower than 0.640V shot-noise is dominant, and most of the noise arises in the depletion region close to the barrier. At increasing voltages, thermal noise associated with the series resistance prevails, and the noise becomes spatially more distributed, mainly originating from the n region of the device. Finally, at the highest voltages, the presence of hot carriers and intervalley mechanisms in the n region leads to the appearance of an excess noise. In this range, electrons become hot after traveling some distance in the n region. This is the reason why $S_V(0,x;0)$ takes these higher values near the end of the n region.

4. Conclusions

We have presented a microscopic theory of electronic noise in semiconductor materials and devices. Calculations are based on a Monte Carlo simulator which, to include fluctuations of the self-consistent electric field, is coupled with a Poisson solver. Both current and voltage correlation functions and their respective spectral densities are investigated. For the case of homogeneous structures, the presence of hot-carrier conditions is found to couple velocity and energy fluctuations. When considering non-homogeneous structures, the coupling between fluctuations in carrier velocity and self-consistent electric field is proven to essentially modify the noise-spectrum. In particular, the Schottky-diode is analyzed within a microscopic model which naturally describes most of the salient features of its noise spectrum without invoking phenomenological shot and thermal noise sources.

Acknowledgments

This work has been performed within the European Laboratory for Electronic Noise (ELEN) supported by the Commission of European Community through the contracts EKBXCT920047 and ERBCHBICT920162.

Partial support from the SA-14/1492 project by the Consejería de Cultura de la Junta de Castilla y León and by the Italian Consiglio Nazionale delle Ricerche (CNR) is gratefully acknowledged.

References

- /1/ C. Jacoboni and L. Reggiani, *Rev. Mod. Phys.*, **55**, 645 (1983).
- /2/ L. Reggiani, T. Kuhn and L. Varani, *Appl. Phys. A*, **54**, 411 (1992).
- /3/ L. Varani, T. Kuhn, L. Reggiani and Y. Perles, *Solid State Electron.*, **36**, 251 (1993).
- /4/ T. Kuhn, L. Reggiani and L. Varani, *Phys. Rev.*, **B42**, 11133 (1990).
- /5/ P. Lugli and L. Reggiani, *Proceedings of the 8th Int. Conf. on Noise in Physical Systems and 1/f Noise*, Eds. A. D'Amico and P. Mazzetti, North-Holland (Rome, 1985) p. 235.
- /6/ T. Gonzalez, D. Pardo, L. Varani and L. Reggiani, *Appl. Phys. Lett.*, **63**, 84 (1993).
- /7/ J. Zimmerman and E. Constant, *Solid State Electron.*, **23**, 914 (1980).
- /8/ T. Gonzalez, D. Pardo, L. Varani and L. Reggiani, *Appl. Phys. Lett.*, **63**, 3040 (1993).
- /9/ M. Trippe, G. Bosman and A. van der Ziel, *IEEE Trans. Microw. Theory Tech.*, **34**, 1183 (1986).
- /10/ A. Van der Ziel, «*Noise in Solid State Devices and Circuits*», Wiley (New York, 1986).